Unusual COLORED STONES

Recently, a parcel of approximately 40 rare gemstones was submitted to GIA's Carlsbad laboratory for identification. Six of these stones (figure 1) represented gem types that had never been examined at this location. They were identified using standard gemological testing, Raman spectroscopy, and energy-dispersive X-ray fluorescence (EDXRF).

A 0.87 ct translucent green hexagonal step cut was identified as adamite, $Zn_2(AsO_4)(OH)$. It had a specific gravity (SG) of 4.40 and a refractive index (RI) of 1.721–1.750. The stone fluoresced weak green under long-wave UV light but was inert to short-wave UV, which is atypical of adamite. Clouds and fractures were observed with 30× magnification.

A translucent brown trapezoidal step cut with an SG of 5.18 proved to be bahianite, $Al_5SbO_{14}(OH)_2$, which is especially rare as a facet-grade gemstone. The 0.73 ct bahianite had a refractive index over the limit (OTL) of the RI liquid. It was inert under long-wave UV light but displayed very weak blue under short-wave UV light. Large fractures, along with numerous whitish fibrous, radial, and granular inclusions and some surface-breaking opaque metallic inclusions, were visible using 30× magnification. It also displayed vitreous to subadamantine luster.

Figure 1. These rare gemstones were recently examined at GIA's Carlsbad laboratory. From left to right: a 0.87 ct green adamite, a 0.73 ct brown bahianite, a 42.08 ct light brownish yellow cerussite, a 0.33 ct purple chambersite, a 2.45 ct orange olmiite, and a 1.30 ct color-change remondite.

A 42.08 ct transparent light brownish yellow octagonal mixed-cut specimen with an SG of 6.54 displayed an OTL refractive index and a biaxial optic figure, indicating its doubly refractive nature. It was inert to long-wave UV light but fluoresced very weak yellow under short-wave UV light. Magnification revealed strong doubling, strong fire, and numerous growth tubes and needles. Its heft was high due to its lead content. These properties, along with advanced testing, led to its identification as cerussite, $PbCO_3$. Although cerussite is a common weathering product of lead ore minerals, its softness, brittleness, and heat sensitivity make it a very rare faceted gem, particularly in this large size.

Another stone from the collection, a 0.33 ct transparent to semitransparent purple triangle step cut with an SG of 3.49 and an RI of 1.728–1.734, was determined to be chambersite, $Mn_3B_7O_{13}Cl$. The gem was inert to both long- and short-wave UV light and showed numerous clouds with 30× magnification. Chambersite is an extremely rare mineral, found as deep as 70 feet in salt brines (J.E. Arem, "Chambersite," *The Color Encyclopedia of Gemstones*, 1987, 2nd ed., p. 65). Because it is so small and dark, this material is almost never faceted.

A 2.45 ct semitransparent orange cushion modified brilliant was identified as olmiite, $CaMn[SiO_3(OH)](OH)$, which was first discovered in 2006 in

Editors' note: All items were written by staff members of GIA laboratories.

GEMS & GEMOLOGY, Vol. 52, No. 1, pp. 68–76.

South Africa (http://www.mindat.org/min-30762.html). Its SG was 2.95. The stone was doubly refractive, displayed an RI of 1.648–1.671, and fluoresced very weak orangy red under both long- and short-wave UV light. Magnification revealed wavy graining, fibrous dislocations and inclusions, and a slightly oxidized stone surface. Most olmiite crystals are not suitable for faceting.

The final stone of the six, a transparent pear-shaped modified brilliant that changed from greenish yellow under fluorescent light to yellowish orange under incandescent light, was identified as color-change remondite, $Na_3(Ce,La,Ca,Na,Sr)_3(CO_3)_5$. The 1.30 ct stone had an SG of 3.40 and showed an RI of 1.628–1.631, yielding a birefringence of only 0.003. It was inert to both long- and short-wave UV light. Handheld prism spectroscopy revealed a strong rare earth element spectrum. Large growth tubes, scattered particles, and etch channels were observed with 30× magnification. The stone's rounded facet junctions indicated a low hardness. Remondite was previously reported as a color-change burbankite-related mineral from Quebec (Winter 1992 GNI, pp. 270–271).

Such a suite of gemstones, prized among avid gem collectors, is not often submitted to the laboratory. Without the help of advanced analytical equipment such as Raman spectroscopy and EDXRF to complement standard gemological testing, it would be challenging to conclude the identity of these rare gemstones.

Rebecca Tsang

DIAMOND

Inclusion with Radiation Halo

Radiation is known to impart green or brown coloration to diamond. This effect most commonly appears as colored spots, presumably where radioactive mineral grains settled against the diamond for an extended period. Circulation of radioactive groundwater may contribute to a "skin" with more evenly distributed color. In either case, the radiation comes from an external source. GIA's New York lab recently examined a 0.49 ct Fancy pink brown diamond containing an inclusion with a brown radiation stain in the form of a halo (figure 2). In this case, the radiation originated from the inclusion itself.

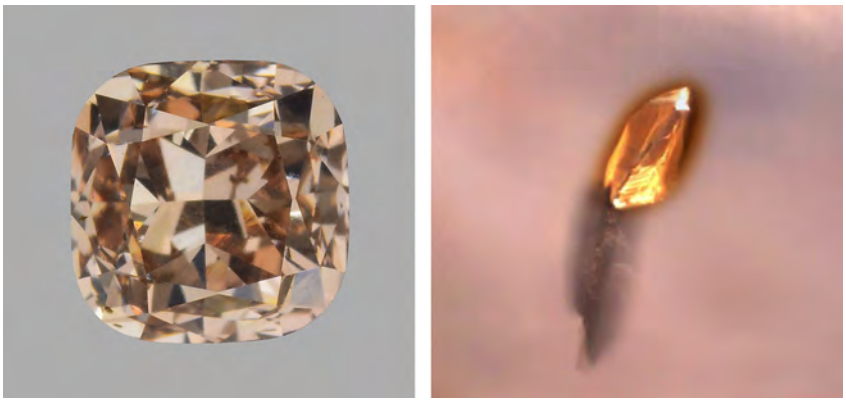

Figure 2. Left: This 0.49 ct Fancy pink brown diamond, measuring 4.11 mm wide, contains a monazite inclusion with a brown radiation halo. Right: A photomicrograph of the monazite inclusion shows the halo thickness of about 10–20 µm. The inclusion's color is masked by the brown radiation stain, but it appears to be yellow or colorless. The dark feature extending from the bottom of the inclusion is a graphitized crack. Field of view 0.36 mm.

Because the inclusion is completely enclosed within the diamond, the material must have been trapped during diamond growth in the mantle. Raman spectroscopy (figure 3) revealed the inclusion to be monazite, $(Ce,La,Nd,Th)PO_4$, a mineral capable of carrying significant amounts of radioactive thorium. Xenotime, YPO_4, a similar rare earth phosphate, has also been reported as an inclusion in diamond with a radiation stain (Fall 2014 Lab Notes, pp. 237–238), but that in-

Figure 3. A Raman spectrum of the inclusion with a radiation halo shows a strong peak at 972 cm^{-1} and smaller peaks at 575 and 415 cm^{-1}, all of which correspond to monazite.

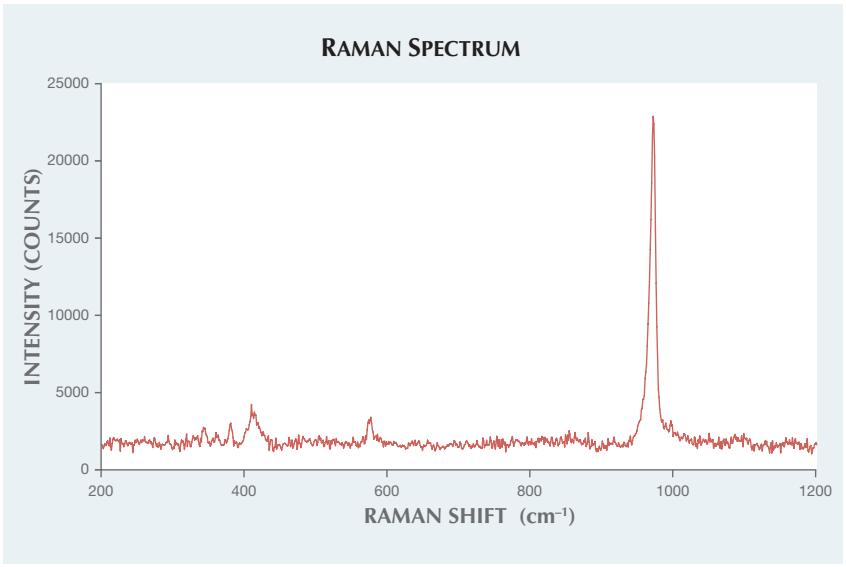

clusion was interpreted as epigenetic.

Monazite is very rarely reported as an inclusion in diamond. It is not part of the common mineral assemblage of peridotitic or eclogitic mantle host rocks. Instead, a rare earth element–enriched phosphate like monazite could be attributed to carbonatitic fluid or melt that infiltrated the host rocks and contributed to diamond growth. Monazite found within peridotite mantle xenoliths has also been ascribed to carbonatitic metasomatism (R.L. Rudnick et al., "Carbonatite metasomatism in the northern Tanzanian mantle: Petrographic and geochemical characteristics," *Earth and Planetary Science Letters*, Vol. 114, No. 4, 1993, pp. 463–475). Other phosphate minerals, chiefly apatite, can be found as a component of the fluid microinclusions that characterize so-called fibrous diamond. Diamond-forming fluids or melts are believed to be an important source of incompatible elements that may reenrich the otherwise depleted refractory lithospheric mantle.

Evan M. Smith and Surjit Dillon Wong

Analysis of Yellow Diamond Melee for Color Treatment and Synthetics

Due to the size and quantity of diamond melee in a parcel, gemological analysis is usually not performed on each specimen. As a result, treated and synthetic diamonds are sometimes mixed with natural diamond melee in parcels (Winter 2014 Lab Notes, pp. 293–294).

Some gemological laboratories are able to properly identify treated and synthetic diamond melee with a combination of infrared absorption spectroscopy, photoluminescence (PL) spectroscopy, and DiamondView fluorescence imaging. GIA's New York laboratory recently tested two parcels of yellow diamond melee submitted for this screening. The results of their examination highlight the importance of laboratory analysis to correctly establishing the nature and color origin of diamond melee.

A parcel of six yellow melee (figure 4), each weighing approximately 0.12 ct, was submitted to GIA for testing. Examination confirmed that all six were natural diamonds treated by HPHT (high-pressure, high-temperature) processing. A combination of mid-infrared absorption spectroscopy (4000–400 cm^{-1}) and PL spectroscopy with 633 nm laser excitation was used to detect this HPHT treatment. Spectroscopic analysis in the mid-IR range revealed the presence of isolated single nitrogen impurities. Four stones contained both A- and B-aggregated nitrogen where the B-aggregate was dominant, while the remaining two contained B-aggregated nitrogen; all six contained isolated single nitrogen. PL spectroscopy revealed features that confirmed these were HPHT-treated diamonds.

Another parcel of 20 yellow diamond melee (figure 5), each weighing between 0.01 and 0.02 ct, was submitted for testing. Mid-IR absorption spectroscopy and DiamondView imaging revealed that three were untreated natural diamonds and one was an HPHT-treated natural diamond; the rest were HPHT synthetics (figure 6). Mid-IR spectroscopy also revealed that 17 of the melee were dominated by A-aggregated nitrogen, three contained both A- and B-aggregated nitrogen, and all 20 contained isolated single nitrogen. The DiamondView images revealed characteristic growth features that helped separate the HPHT synthetic and HPHT-treated material from the natural stones. The HPHT synthetics contained typical cuboctahedral growth patterns, while growth patterns associated with natural diamond formation were observed in the natural diamonds, both untreated and HPHT-treated.

Figure 4. These six melee were revealed to be HPHT-treated natural diamonds.

Figure 5. Of this group of 20 diamond melee, 16 were HPHT synthetics (left). Three were untreated natural diamonds (center), and one was an HPHT-treated natural diamond (right).

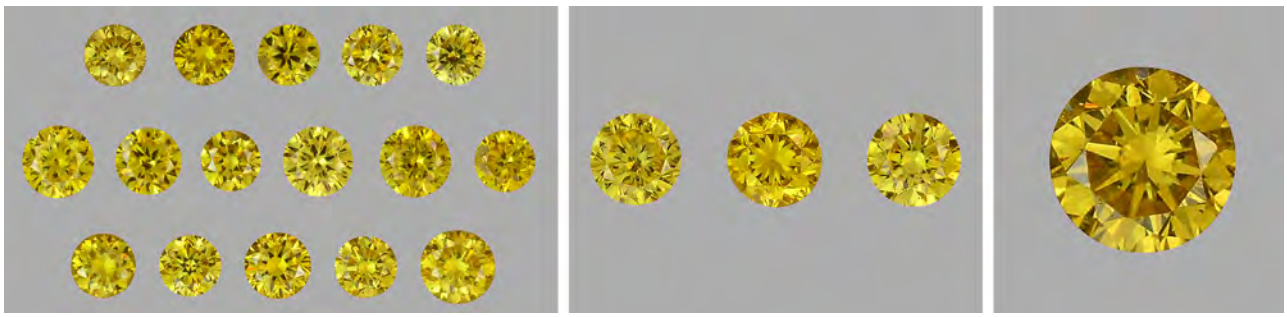

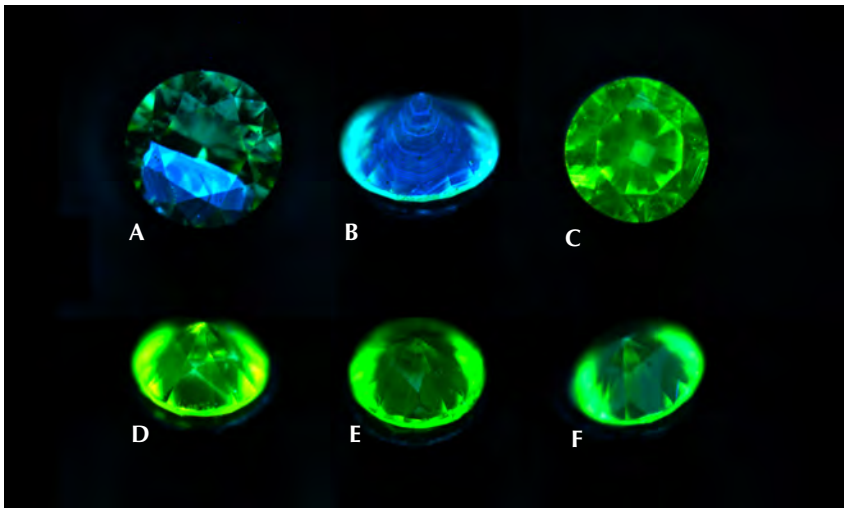

Figure 6. These DiamondView images show characteristic growth features typical of (A) untreated natural, (B) HPHT-treated natural, and (C–F) HPHT synthetic diamond.

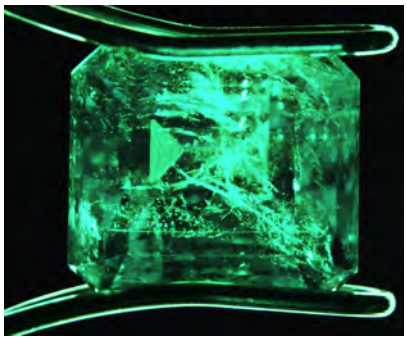

Figure 7. This 1.81 ct specimen was a natural emerald/emerald doublet. Field of view 10.5 mm.

This analysis highlights the importance of laboratory testing to correctly identifying the nature and color origin of diamond melee, and to minimizing the risk of mixing treated and synthetic diamonds with natural melee in the marketplace.

Caitlin Dieck, Manisha Bhoir, and Paul Johnson

EMERALD/Emerald Doublet

While various combinations of materials are used to form doublet gems, we seldom see doublets consisting of the same materials. Ruby/ruby doublets (Spring 1987 Lab Notes, pp. 47–48; Spring 1996 Lab Notes, p. 49) as well as a tourmaline/tourmaline doublet (Summer 1990 GNI, pp. 165–166) have been reported, but a doublet consisting of two sections of natural emerald has not been previously documented.

GIA's Tokyo laboratory recently examined a 1.81 ct transparent green octagonal step cut that measured approximately 7.22 × 6.71 × 5.55 mm (figure 7). Standard gemological testing indicated an SG of 2.71, with an RI of 1.572–1.580 on the crown and 1.570–1.578 on the pavilion. A chromium spectrum consistent with emerald was visible with a handheld spectroscope. Upon first glance, this stone appeared to be a natural Colombian emerald, but careful examination easily revealed its doublet nature, while Raman spectroscopy confirmed that both the top and bottom portions were indeed beryl.

Microscopic observation revealed a very flat separation plane below the girdle, crossing the pavilion diagonally. Flattened gas bubbles were visible along the plane (figure 8, left), and a blue and orange flash effect was also apparent. Jagged three-phase inclusions typical of Colombian emeralds were visible in both parts, while fine growth tubes and fingerprints in helix patterns were seen only in the top portion. Inclusions did not cross the boundary between the two sections. Under long-wave UV light, the top showed a stronger red fluorescence than the bottom, with a distinct boundary between the two (figure 8, right). A whitish fluorescence was also observed along the plane. Illumination using crossed polarizers revealed that the top and bottom portions had different optical orientations, with two optic axes visible (figure 9). Typical of most emeralds, enhanced fractures showing a flash effect were found in both parts.

Immersion with methylene iodide revealed green angular zoning in the bottom, whereas the top had even, saturated green color. Both sections appeared to have enough green color to be considered emerald. The glue along the separation plane was color-

Figure 8. Left: Flattened gas bubbles are visible along the separation plane of the doublet. Field of view approximately 3 mm. Right: Viewed under long-wave UV light, the doublet displayed strong red fluorescence in the top portion but not the bottom. A distinct boundary between the two parts is clearly visible.

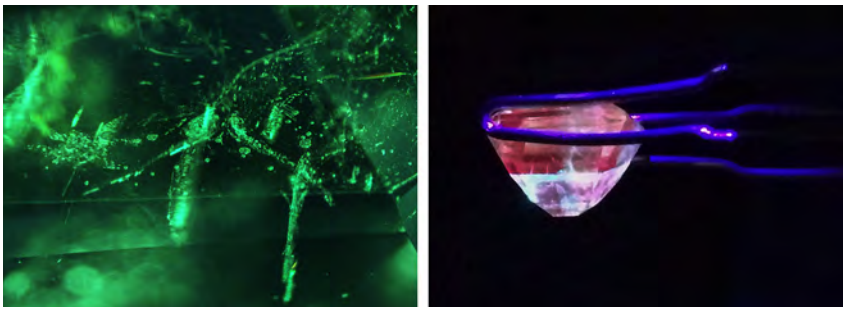

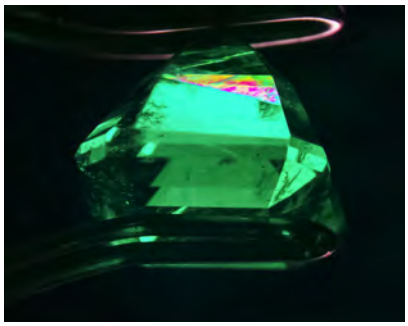

Figure 9. When the doublet was viewed under crossed polarizers, different optical orientations were apparent. At this angle, interference colors along the optic axis are clearly visible in the bottom portion but not the top. Field of view 11.60 mm.

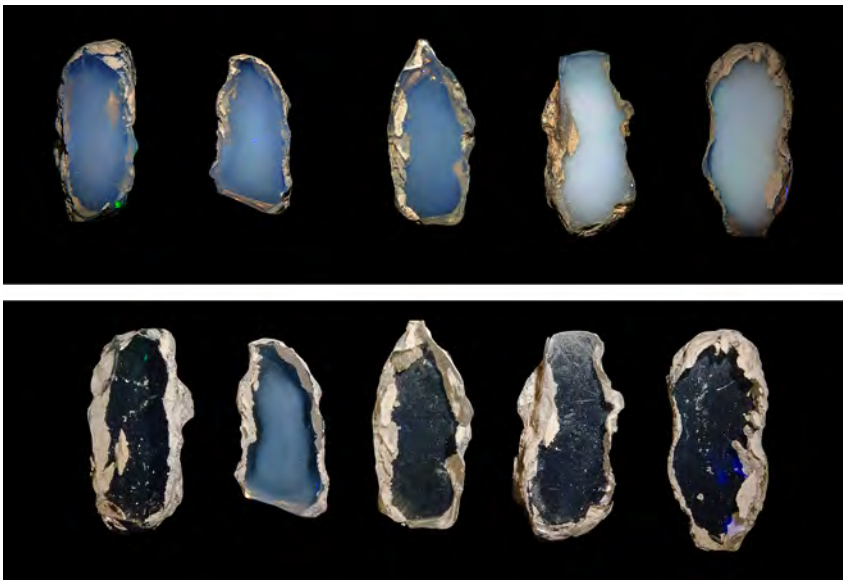

Figure 10. Top: These five opal slices of comparable thickness were cut from the same rough. They were semitransparent to translucent when viewed in daylight on a black background. Play-of-color was displayed with oblique lighting at certain angles. Bottom: The slices' transparency improved after immersion in distilled water for approximately 20–30 minutes. Each slice absorbed water differently depending on its porosity.

less. This is unusual, as assembled imitations of emerald are often composed of pale beryl or other colorless materials with a green cement layer. We could only speculate on the circumstances leading to the creation of this unusual doublet.

Yusuke Katsurada and Claire Ito

Hydrophane OPAL Treatments

Recently in GIA's Bangkok lab, an approximately 4 cm piece of rough hydrophane opal was fabricated into five slices for various treatment experiments. Each slice was approximately 0.5 cm thick. Only clean tap water was used in the cutting process, and no other materials besides opal were involved. The opal slices showed a whitish, cloudy appearance in daylight and appeared light brown to brown in calibrated diffused light.

After the cutting step, all five slices underwent specific gravity testing, which gave SG values of approximately 1.93 ±0.03. While immersed in water, the slices displayed obvious weight gain and improved transparency, which indicated that the material was hydrophane opal (figure 10).

TABLE 1. Appearance of hydrophane opal slices before and after treatment.

	Oil treatment		Opticon treatment	
	Before	After	Before	After
Daylight	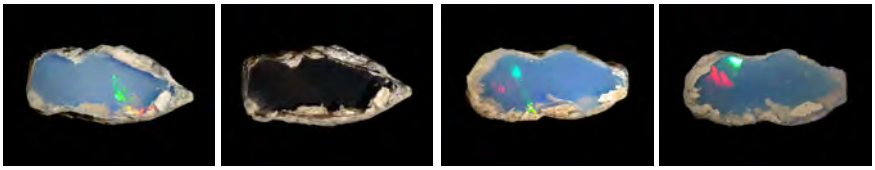			
Calibrated transmitted light				

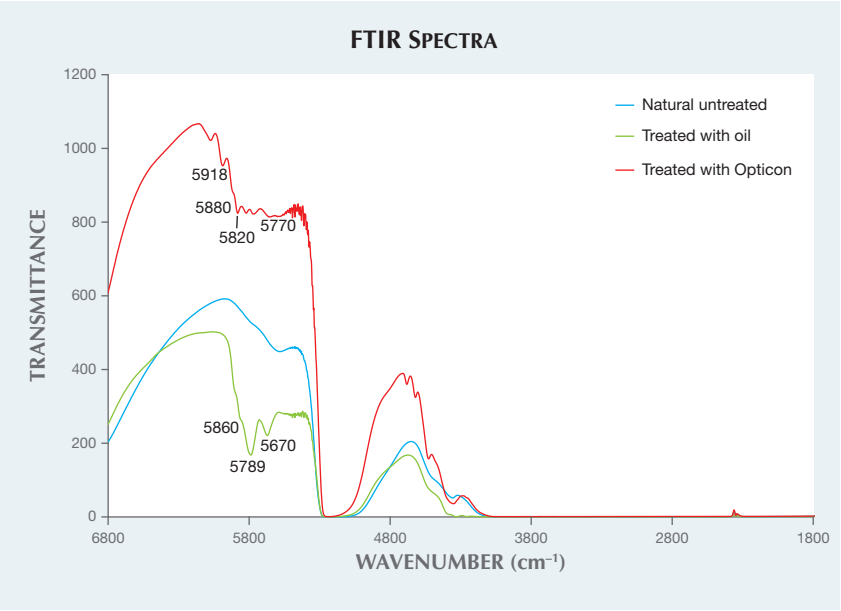

Figure 11. FTIR spectra of untreated, oil-treated, and Opticon-treated opal. The two treated opals show characteristic FTIR peaks in the 5600–5900 cm^{-1} range, while untreated opal does not show any peaks in this range.

The water-absorbing ability of the opal was found to vary through the whole piece, resulting from its non-uniform porosity, and could be calculated as percentage weight changes in water, ranging from 5% to 13%. It took approximately one week to restore the opal's original weight and appearance.

Two slices were then selected for oil and Opticon treatment experiments. The treatment procedures were identical. The pieces of opal were heated to approximately 80°C and then placed in warm oil or Opticon of the same temperature under vacuum conditions. They were heated continuously for 15 to 20 minutes, which was indicated by the presence of gas bubbles on the opal. Once the slices had fully absorbed the oil or Opticon, there were few, if any, gas bubbles. Afterward, the slices were removed, cleaned with a dry cloth, and left to air-dry overnight at room temperature.

Both treated opal slices were analyzed using a gemological microscope and advanced instruments. Oil treatment improved transparency but destroyed play-of-color (table 1, left). Opticon treatment enhanced transparency while preserving play-of-color (table 1, right). The FTIR spectrum of the oil-treated slice showed oil-related peaks at 5670, 5789, and 5860 cm^{-1}, whereas the FTIR spectrum of the Opticon-treated slice displayed a series of related peaks in the 5600–5900 cm^{-1} range (figure 11). Raman spectra also demonstrated the presence of treatments. The oil-treated sample displayed peaks at 2929, 2897, 2873, 2851, and 2724 cm^{-1}, while the Opticon-treated slice showed dominant peaks at 3071, 2931, and 2873 cm^{-1}, and a series of smaller peaks in the 600–1600 cm^{-1} range (figure 12).

While oil and Opticon are not easily observed with the unaided eye or even with a microscope, they are readily detected by advanced instruments. Using Opticon, the process could be combined with other treatments, such as dyeing or sugar-acid treatment, to improve the durability and transparency of opal.

Ratima Suthiyuth and Vararut Weeramonkhonlert

Figure 12. Raman spectra of untreated, oil-treated, and Opticon-treated opal. The oil-treated opal shows characteristic Raman peaks at 2929, 2897, 2873, 2851, and 2724 cm^{-1}. The Opticon-treated opal displays characteristic Raman peaks at 3071, 2931, and 2873 cm^{-1}, with a series of smaller peaks in the 600–1600 cm^{-1} range.

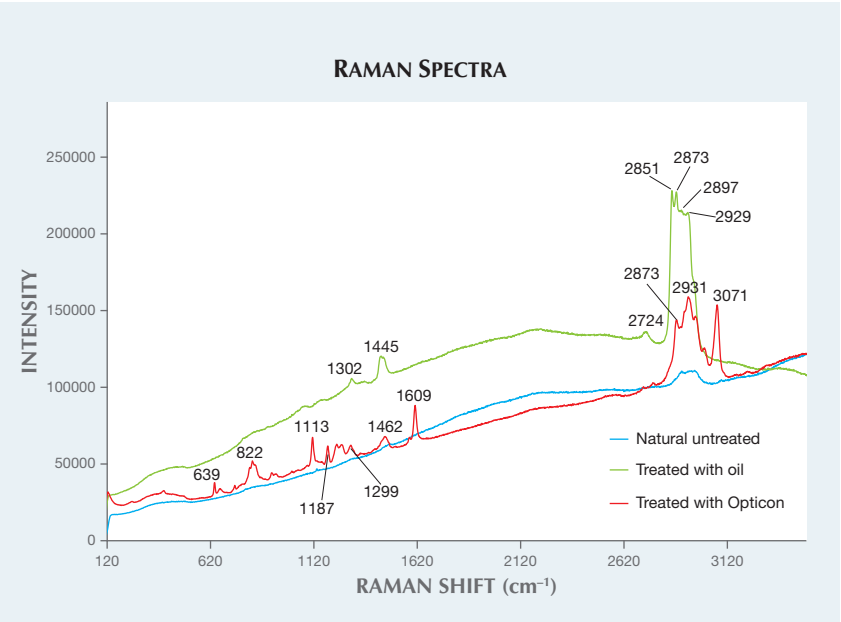

Figure 13. A 5.03 ct Fancy Deep blue HPHT synthetic diamond was examined by GIA (left). Faint but sharp color zoning was observed (middle, field of view 4.77 mm), along with small metallic inclusions and a cavity at the girdle (right, field of view 2.19 mm).

SYNTHETIC DIAMOND

Largest Blue HPHT Synthetic

Recently, large colorless and near-colorless HPHT-grown diamonds by the Russian company NDT have been investigated, with sizes up to 5.11 ct (U. D'Haenens-Johansson et al., "Large colorless HPHT-grown synthetic gem diamonds from New Diamond Technology, Russia," Fall 2015 *G&G*, pp. 260–279; Spring 2015 *G&G* Lab Notes, pp. 65–66). The largest faceted colorless HPHT-grown synthetic diamond reported to date is a 10.02 ct E-color, VS_1-clarity specimen, reported by IGI Hong Kong in 2015. In January 2016, GIA's New York laboratory examined a 5.03 ct fancy-color HPHT-grown type IIb synthetic diamond (figure 13, left) produced by NDT, the largest faceted blue laboratory-grown diamond studied so far.

This emerald-cut synthetic diamond was color graded as Fancy Deep blue. This is a very attractive color with no other color component, a prized rarity among natural type IIb diamonds (the Blue Moon, for instance, was graded as Fancy Vivid blue). When viewed using a microscope, faint but sharp color zoning could be seen (figure 13, center), indicative of the uneven impurity incorporation of HPHT synthetic diamonds. No strain was observed under crossed polarizers, indicating a very low dislocation density, which is also characteristic of HPHT-grown diamonds. It had VS_1 clarity, with only very small metallic inclusions and a cavity observed at the girdle (figure 13, right). Fluorescence and phosphorescence images collected using a DiamondView instrument revealed the sample's cuboctahedral growth pattern (figure 14, left), another feature of HPHT synthetics. The long-lasting chalky blue phosphorescence was further analyzed using spectroscopy, and the emission was found to originate from two broad bands centered at approximately 500 and 575 nm (figure 14, right). These bands have previously been reported in NDT's type IIa and IIb HPHT synthetic diamonds (D'Haenens-Johansson et al., 2015).

Figure 14. DiamondView images of fluorescence (top left), and phosphorescence (bottom left) revealed a cuboctahedral growth pattern, which is typical for HPHT-grown synthetic diamond. Phosphorescence spectra (right) show two peaks at approximately 500 and 575 nm, contributing a chalky blue color.

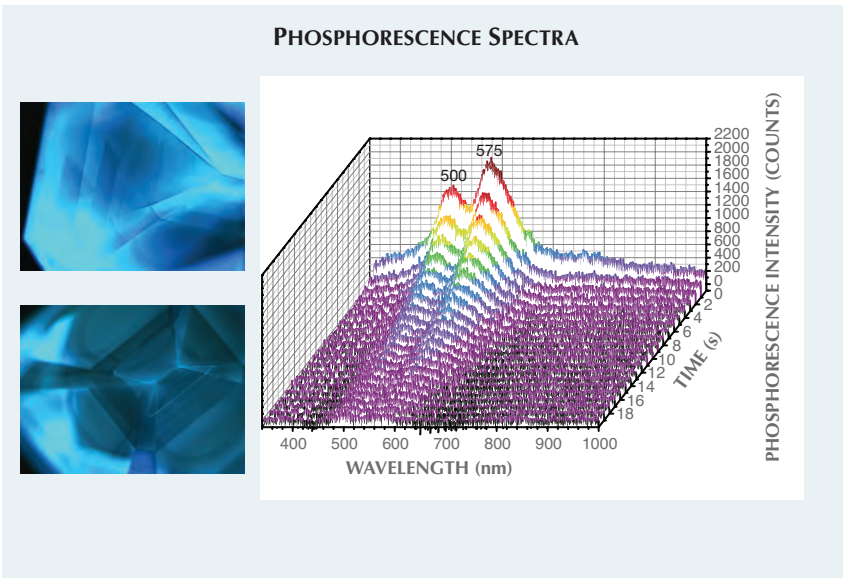

Absorption spectroscopy for the mid-infrared region confirmed the sample was type IIb, with strong boron-related features at 1290, 2458, and 2800 cm^{-1}. The average bulk boron concentration was 0.82 to 1.12 ppm, calculated according to the equation N_A-N_D = (1.00 ± 0.15) × H_{1290} ppm cm^{-3}, where N_A is acceptor concentration, N_D is donor concentration, and H_{1290} is peak height at 1290 cm^{-1} (A.T. Collins, "Determination of the boron concentration in diamond using optical spectroscopy," *Proceedings of the*

61st Diamond Conference, Warwick, UK, 2010). Otherwise, this large synthetic diamond exhibited an extremely low concentration of optical defects. PL spectroscopy was conducted at liquid nitrogen temperatures using a range of laser excitations covering the UV-visible-IR range. The PL spectra only revealed emission from a single defect species, a Ni-related emission multiplet with peaks at 483.6/483.8/484.1/484.4 nm (484 nm center) detected using 324.8 nm laser excitation (A.T. Collins, "The characterisation of point defects in diamond by luminescence spectroscopy," *Diamond and Related Materials*, Vol. 1, 1992, pp. 457–469). As with previous type IIb synthetic diamonds, its visible-NIR spectrum showed a transmission window in the blue region and an absorption in the red, caused by the presence of boron, resulting in the observed blue bodycolor.

This 5.03 ct sample is the largest HPHT-grown blue synthetic diamond examined at a GIA laboratory. As the size and quality of synthetic diamonds improve, careful identification is essential. Representative HPHT synthetic diamond characteristics seen in this specimen, such as the lack of tatami strain patterns (which are typically observed in natural type IIb diamonds), faint but sharp color zoning, and small metallic inclusions from the metal-catalyst flux, can be detected using a gemological microscope, emphasizing its continued importance in gem identification. Examination of this large IIb synthetic diamond, combined with those previously reported from NDT, illustrates the rapid progress in HPHT growth technologies. This is a development that will eventually impact the jewelry industry.

Kyaw Soe Moe, Paul Johnson, Ulrika D'Haenens-Johansson, and Wuyi Wang

Ring with a CVD Synthetic Melee

The separation of synthetic diamond melee from natural diamond melee is a significant concern. Some specimens have been identified by GIA and other laboratories as synthetic, but those products were predominantly HPHT grown. GIA's Hong Kong lab recently identified a CVD synthetic melee mounted in a ring (figure 15).

Figure 15. One of the round-cut melee mounted in this ring was identified as a CVD synthetic diamond.

The round-cut synthetic measured approximately 2.8 mm in diameter and weighed about 0.08 ct. Color could not be graded due to the mounting, but it was estimated to be in the F-H range. The material showed no notable visual features using the microscope other than a small surface scratch at the table. Infrared absorption spectroscopy indicated the typical features of a type IIa diamond; no defect-related absorption feature was detected. A PL spectrum was collected at liquid nitrogen temperature with a very wide range of laser excitation wavelengths. Major features included emissions from [N-V] and [Si-V]$^-$ centers (figure 16). The emission at 575.0 nm from [N-V]^0 is much stronger than the peak at 637.1 nm from [N-V]$^-$, similar to many natural type IIa diamonds. Most notably, this specimen showed very strong emissions at 736.6 and 736.9 nm from the [Si-V]$^-$ defect. Using 514 nm laser excitation, the intensity of the [Si-V]$^-$ defect was about eight times that of the diamond Raman line. DiamondView imaging revealed strong orange color with small irregular areas of blue fluorescence (figure 17). All these observations confirmed that this melee is an as-grown CVD synthetic.

This was the first mounted CVD synthetic melee diamond identified by GIA. While synthetics of this size

Figure 16. The photoluminescence spectrum collected at liquid nitrogen temperature with 514 nm laser excitation shows moderate emissions from [N-V] centers and a very strong emission from [Si-V]$^-$.

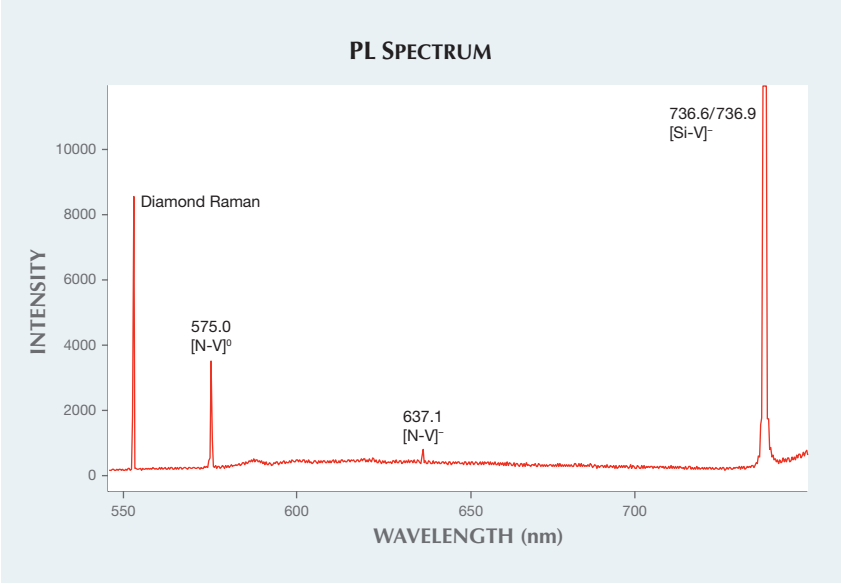

Figure 17. DiamondView imaging showed strong orange fluorescence with small irregular areas of blue fluorescence, a typical feature of as-grown CVD synthetic diamond.

are overwhelmingly HPHT grown, we do expect to see more CVD synthetic diamond melee in the future.

Terry Poon, Carmen Lo, and Billie Law

Quench-Crackled Blue SYNTHETIC SPINEL

Recently, GIA's Bangkok laboratory examined an interesting 9.75 ct blue oval mixed cut (figure 18). Standard gemological properties included an RI of 1.728, with strong anomalous double refraction using the polariscope. The sample's Chelsea filter reaction exhibited a strong red transmission, and absorption bands at 540, 580, and 635 nm were seen in the handheld spectroscope. The specimen fluoresced strong red under long-wave UV radiation and strong bluish white under short-wave UV. These properties are diagnostic features of cobalt blue synthetic spinel grown by the Verneuil (flame-fusion) process.

Microscopic observation revealed tiny strings of gas bubbles and strong irregular graining, with many reflective fractures on one side of the sample (figure 19). The specimen appeared

Figure 18. A 9.75 ct synthetic spinel, seen in GIA's Bangkok lab, was proven to be treated by the quench-crackling method.

to have been heated and thermally shocked. This method, known as quench-crackling, typically involves the use of a dye to create a preferable color, but not in this specimen. While DiamondView imaging showed clear fractures similar to those found in quench-crackled treated material (figure 20), a PL spectrum of Cr^{3+} shifted from 685 to 689 nm was consistent with synthetic spinel (S. Saeseaw et al., "Distinguishing heated spinels from unheated natural spinels and from synthetic spinels," GIA Research News, April 2009).

Laser ablation–inductively coupled plasma–mass spectrometry (LA-ICP-MS) was utilized for a trace element analysis. The results displayed high amounts of Co (up to 167 ppma), along with 1137 ppma Ti and 337 ppma Cr. Zn was found with a maximum of 6 ppma, and Ga was below the detection limit. This specimen contained higher amounts of Ti and Co than those previously reported in S. Saeseaw et al. ("Cobalt diffusion of natural spinel: A report describing a new treatment on the gem market," GIA Research News, June 2015). We concluded that a quench-crackling technique was used to make the synthetic spinel appear more like a natural spinel. In such cases, standard gemological properties are useful for accurate identification.

Figure 19. These reflective fractures were seen in the blue synthetic spinel. Field of view 2.5 mm.

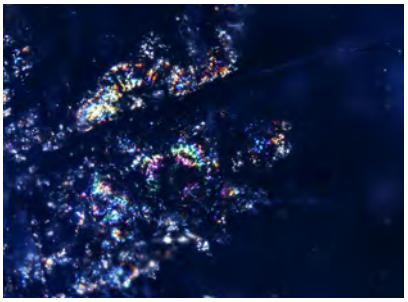

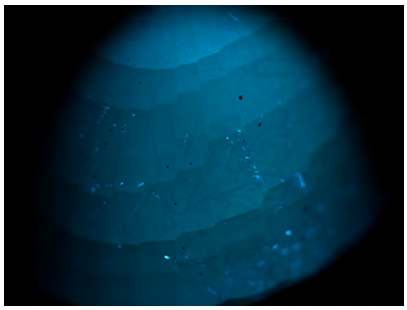

Figure 20. DiamondView imaging of the synthetic spinel showed fractures typical of quench-crackled material.

Sudarat Saeseaw and Charuwan Khowpong

PHOTO CREDITS:
C.D. Mengason—1; Jian Xin (Jae) Liao—2 (left), 5; Evan Smith—2 (right); Sood Oil (Judy) Chia—4, 13 (left); Manisha Bhoir—6; Claire Ito—7, 9; Ahmadjan Abduriyim—8; Nuttapol Kitdee—10, 18; Kyaw Soe Moe—13 (center and right), 14; Johnny Leung—15; Carmen Lo—17; Charuwan Khowpong—19, 20; Sasithorn Engniwat—table 1.